

## First-principles study of the geometry of Ag nanowires growing on a self-assembled Bi nanoline

This article has been downloaded from IOPscience. Please scroll down to see the full text article.

2007 J. Phys.: Condens. Matter 19 365225

(<http://iopscience.iop.org/0953-8984/19/36/365225>)

View [the table of contents for this issue](#), or go to the [journal homepage](#) for more

Download details:

IP Address: 129.252.86.83

The article was downloaded on 29/05/2010 at 04:37

Please note that [terms and conditions apply](#).

# First-principles study of the geometry of Ag nanowires growing on a self-assembled Bi nanoline

H Koga and T Ohno

Computational Materials Science Center (CMSC), National Institute for Materials Science (NIMS), 1-2-1 Sengen, Tsukuba, Ibaraki 305-0047, Japan

E-mail: [koga.hiroaki@nims.go.jp](mailto:koga.hiroaki@nims.go.jp) and [ohno.takahisa@nims.go.jp](mailto:ohno.takahisa@nims.go.jp)

Received 30 November 2006

Published 24 August 2007

Online at [stacks.iop.org/JPhysCM/19/365225](http://stacks.iop.org/JPhysCM/19/365225)

## Abstract

Epitaxial Ag nanowires on a self-assembled Bi nanoline on the Si(001) surface are examined for their geometry and energetic stability at the level of the generalized-gradient approximation. The orientations examined are Ag(001)[100], Ag(110)[100], Ag(111)[110], and Ag(001)[110], where the indices refer to the plane and the direction parallel to the Si(001) surface and the Bi nanoline, respectively. The wires are found to have mostly bulklike structure, except that Ag(001) monolayers undergo extensive reconstruction. The calculated electronic band structure indicates that the Ag wires are metallic wires. Particularly stable among the wires are the Ag(111) wires, having a coincident site lattice interface with the Bi nanoline. The energetic stability generally improves with thickness, indicating that Ag grows through three-dimensional nucleation on the Bi nanoline.

(Some figures in this article are in colour only in the electronic version)

## 1. Introduction

New methods to create nanowires [1] are intensively studied because of great scientific and technological interest in their electronic, magnetic, and optical properties. Nanowires are typically prepared using lithographic techniques or through self-assembly. Alternatively, nanowires may be grown using other self-assembled nanostructures as templates. Among such templates, double lines of Bi dimers (Bi nanolines) [2, 3] self-assembled on the Si(001) surface are particularly interesting to surface physicists: according to a recent report [4], Ag adsorbed preferentially on the Bi nanolines, forming small dots ( $\sim 1$  nm) and also beginnings of a nanowire (figure 4 in [4]); furthermore, indium also adsorbed on the Bi nanolines, forming nanoislands elongated along the Bi nanolines [5]. (In these experiments, ammonia was used to passivate the Si(001) surface. Without passivation, the preferential adsorption did not occur [6].)

The Bi nanoline is also an active topic in the field of quantum simulation. Density-functional theory (DFT) and tight-binding calculations were essential in clarifying its atomic structure [7]. DFT calculations [8] have also predicted that a one-dimensional array of Fe atoms on the Bi nanoline shows a magnetic half-metal behaviour. In our previous first-principles studies [9, 10], we have found that a Ag (Au) atom adsorbs preferentially on the Bi nanoline, entering its Bi–Si backbond (figure 4(a) in [9]). This supports the idea of using the Bi nanoline as a template for Ag (Au) nanostructures.

In this first-principles study, we focus on the geometries and energies of epitaxial Ag nanowires on the Bi nanoline. The wires examined here have a width (three Ag atoms) comparable to that of the Bi nanoline (0.6 nm), occupy the Bi–Si backbond sites, and thus sit directly on Si. We examine Ag(001)[100], Ag(110)[100], Ag(111)[110], and Ag(001)[110] wires, where the indices refer to the plane and the direction parallel to Si(001) and the Bi nanoline (namely the Si[110] direction), respectively. Along the Ag[100]  $\parallel$  Si[110] direction, two Ag atoms match two Si atoms and a Bi dimer with a 6% mismatch. Along the Ag[110]  $\parallel$  Si[110] direction, eight Ag atoms almost exactly match six Si atoms and three Bi dimers, thus forming a coincident site lattice (CSL) interface; such an interface appears in a Ag/Si(001) heteroepitaxy [11]. The Ag[100] wires we examined have Ag(001) facets, while the Ag[110] wires have Ag(111) facets; these facets are the highest in density among those parallel to Ag[100] and Ag[110], respectively, and are thus more likely to appear under growth conditions. For these wires, we discuss the geometry, the relative stability, and the variation of energetic stability with thickness, and find the following features. First, except Ag(001) monolayers, the Ag wires have bulklike structure. The heights of the wires are thus very close to multiples of a bulk interplanar spacing. This facilitates the identification of the Ag wires using measured heights. Second, the electronic band structure indicates that the wires are metallic wires. Third, the Ag(111)[110] wires, with an excellent CSL interface, are particularly stable among the wires examined. Last, the energetic stability of the Ag wire generally improves as the thickness increases; such a trend indicates that Ag grows through three-dimensional nucleation rather than layer by layer, according to the thermodynamic criterion of the growth mode [12–14]. (A future publication will discuss the geometry and the growth of Ag nuclei.) These findings form the basis for the understanding of the mechanism of Ag growth on the Bi nanoline, and will also be useful in experiment in identifying the orientation of a wire. This paper is organized as follows. In section 2, calculation methods are explained. In section 3, calculation results are discussed; we first examine the Ag[100] wires and then the Ag[110] wires; thereafter, we discuss the variation of the height and the energetic stability with thickness. In section 4, the results will be summarized.

## 2. Method

The optimized geometries and their energies reported in this paper are calculated within the generalized-gradient approximation (GGA) [15] using a density-functional [16, 17] plane-wave pseudopotential code.<sup>1</sup> The calculation conditions differ from those used in our previous study [9] in the size of the unit cell and the density of the  $k$ -point grid; the Ag[110] wires are calculated using a  $6 \times 6$  cell with the  $1 \times 2$  grid, and the Ag[100] wires using a  $6 \times 2$  cell with the  $1 \times 6$  grid. The energetic stability of a Ag wire is expressed in terms of the adsorption potential energy ( $E_a$ ), defined according to (1) in [9]. The coverage of 1.0 is defined as the Ag number density in the Ag(111)[110] monolayer (see figure 4(a) below), which is eight Ag

<sup>1</sup> Simulation Tool for Atom TEchnology (STATE) version 5.01, Research Institute for Computational Sciences (RICS), National Institute of Advanced Industrial Science and Technology (AIST), 2002.

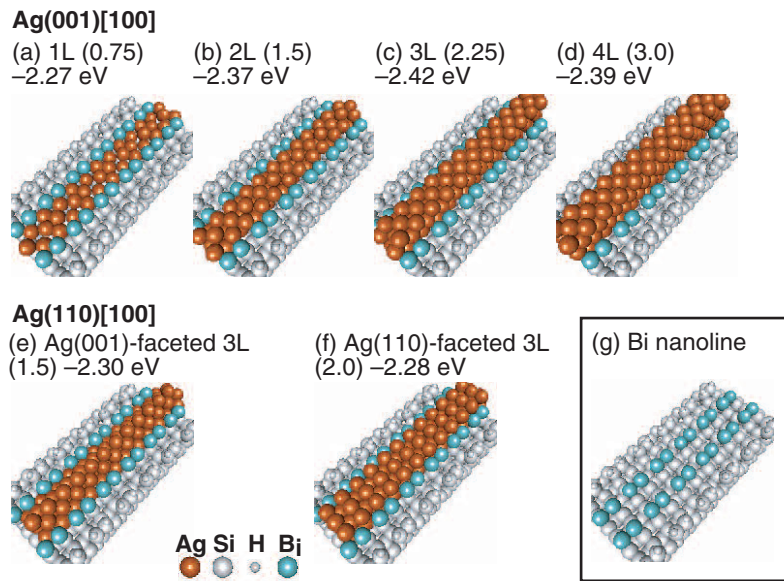


**Figure 1.** (a)–(f) Optimized geometries of Ag[100] wires (perspective view) and their energies  $E_a$  (eV). Numbers in parentheses are coverages. The 5 L and 6 L Ag(001)[100] wires are not shown. (g) Bi nanoline.

**Table 1.** Variation of the adsorption potential energy  $E_a$  (eV) of the Ag(001)[100] 3 L wire (figure 1(c)) with calculation conditions.  $N_l$  denotes the number of Si(001) layers in the slab.

Cell	$N_l$	$k$ -point	$E_a$	
$6 \times 2$	6	$1 \times 6$	-2.420	Present (short cell)
$6 \times 6$	6	$1 \times 2$	-2.419	Present (long cell)
$6 \times 2$	6	$1 \times 8$	-2.420	More $k$ points
$8 \times 2$	8	$1 \times 6$	-2.415	Larger model

atoms per unit cell of the Bi nanoline. The height is measured from the top of the Bi nanoline before Ag adsorption.

To assess the accuracy of the calculation, the adsorption potential energy  $E_a$  of the Ag(001)[100] 3 L wire (see figure 1(c)) was calculated under various calculation conditions. The results are listed in table 1. As this table shows, the  $6 \times 6$  cell gives essentially the same energy as the  $6 \times 2$  cell, so the energies obtained using the two different cells can be directly compared. Furthermore, changing the density of the  $k$ -point grid or the model size (namely, width and slab thickness) has negligible effect on the calculated energy. Finally, increasing the cut-off energy to 20 Ryd changes the difference in  $E_a$  between the 2 L and the 3 L Ag(001)[100] wires by no more than 4 meV (not shown in the table). Thus, an energy difference of  $\sim 0.01$  eV is considered significant in the following discussion.

### 3. Results and discussion

In this section, we first examine Ag(001)[100] and Ag(110)[100] wires and then Ag(111)[110] and Ag(001)[110] wires. Thereafter, we discuss the variation of the height and the energetic stability with thickness.

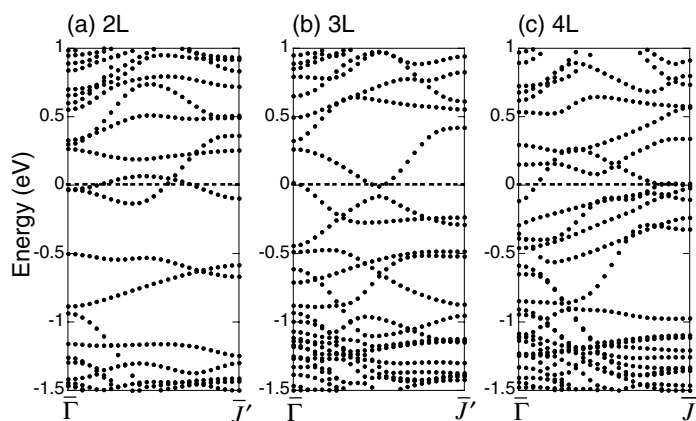


**Figure 2.** Electronic band structure of the Ag(001)[100] wires along the wire direction. The Fermi level is at zero energy.

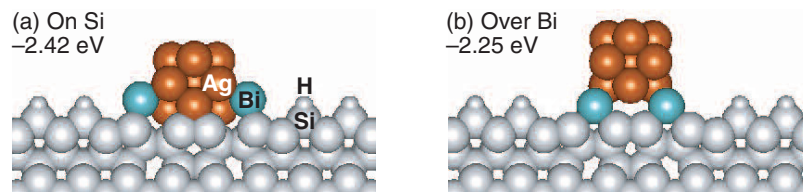
The optimized geometries of the Ag(001)[100] and Ag(110)[100] wires are shown in figures 1(a)–(f). As figure 1(a) shows, the Ag(001) monolayer undergoes significant reconstruction, decomposing into monomer pairs ( $D1D1$  in figure 5 of [9]) and rhombi; the distance from a monomer to its adjacent rhombus (0.323 nm) is much larger than the bulk bond length (0.288 nm). The Ag monomer pair gains energy through an interaction involving the underlying Si atoms [9], and the rhombus over a square through a creation of a bond along its diagonal.

In contrast, the Ag(001) 2 L wire (figure 1(b)) is nearly bulklike, except for a few changes. First, the base layer changes from a square chain into a rhombus chain, with each rhombus oriented perpendicular to its neighbours; the ratio of the diagonal lengths (parallel to Ag[100]) of two adjacent rhombi is 0.72. Such a deformation is necessary to fit the Ag[100] wire to the Bi nanoline, which has twice the periodicity of Ag[100]. This deformation is accompanied by that of the second layer, where every other middle-row atom is raised by 0.036 nm with respect to the rest. Last, the width (0.446 nm) of the second layer is larger than the bulk value (0.408 nm).

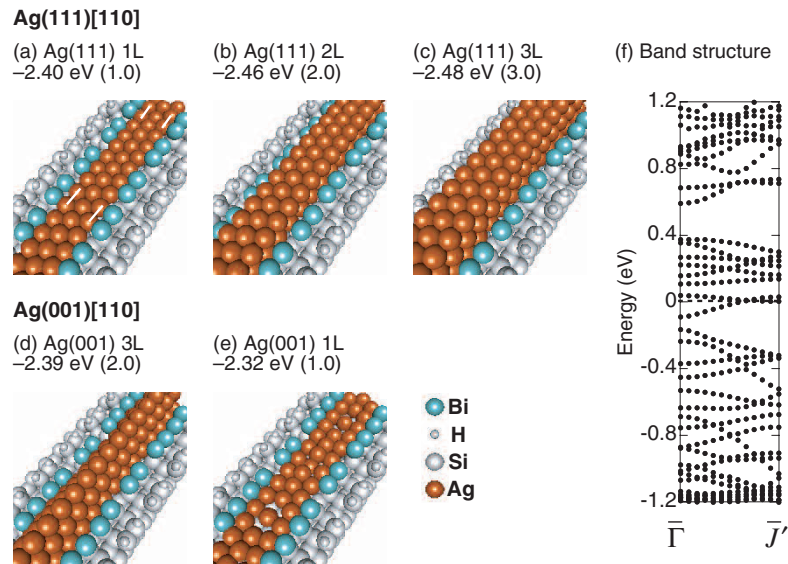
The Ag(001) wires of three to six layers are much more bulklike, as can be seen in figures 1(c) and (d). The width of the top layer (around 0.40 nm), for example, becomes comparable to the bulk value (0.408 nm). Furthermore, the reconstruction of the base layer into a rhombus chain becomes less apparent: the ratio of the diagonal lengths (mentioned above) is around 0.85, which is closer to unity than that (0.72) in the 2 L wire. The wire geometry thus becomes more bulklike as it grows thicker, in accordance with expectation.

Figure 2 shows the electronic band structure of the 2–4 L Ag(001)[100] wires along the wire direction ( $\bar{\Gamma}\bar{J}'$ ). These bands indicate that the wires are metallic (2 L and 4 L) or semimetallic (3 L); as can be seen in the figure, partially filled bands lie within the energy gap of the substrate.

The Ag(001) wires examined above have the Ag/Si interface. To demonstrate the favourableness of this interface, we also calculated the Ag(001) 3 L wire that grows over Bi and thus has no Ag/Si interface (figure 3(b)). This wire is 0.17 eV higher in energy than its on-Si counterpart (figures 3(a) and 1(c)), although the two wires have almost identical structures. It will be, however, very difficult to determine whether the interface is Ag/Si from scanning-tunnelling-microscopy (STM) images alone, because the over-Bi 3 L wire and the on-Si 4 L



**Figure 3.** Ag(001)[100] 3 L wire on Si (a) and that over Bi (b) (viewed from Si[110]).



**Figure 4.** (a)–(e) Optimized geometries of Ag[110] wires (perspective view) and their energies  $E_a$  (eV). Numbers in parentheses are coverages. The Ag(111) 4 L wire is not shown. The Ag–Ag bonds elongated to  $0.302$  nm (see text) are indicated by white lines. (f) Electronic band structure of the Ag(111) monolayer along the wire direction. The Fermi level is at zero energy.

wire (figure 1(d)) have similar heights ( $0.607$  and  $0.632$  nm, respectively) and almost identical facets; the only notable difference is the registry with the background Si dimer rows.

The Ag(110)[100] 3 L wire with Ag(001) facets (figure 1(e)) also shows a bulklike structure, except that its height ( $0.238$  nm) somewhat deviates from the bulk value ( $0.288$  nm). This wire has the same coverage (1.5) and the same number of atoms (six atoms per cell, discounting the base layer) on the Ag(001) facets as the Ag(001) 2 L wire; however, its base layer ( $0.63$  nm wide) is wider than the Ag(001) base layer ( $0.47$  nm wide) and thus does not fit so well to the underlying row of Si–Si bonds ( $0.24$  nm wide). This wire correspondingly has a higher energy ( $-2.30$  eV) than the Ag(001) 2 L wire ( $-2.37$  eV). Similarly, the Ag(110)-faceted Ag(110)[100] 3 L wire (figure 1(f)) has a higher energy ( $-2.28$  eV) than the Ag(001) 2 L wire. It is also higher in energy than the Ag(001)-faceted Ag(110) wire. Thus, changing the facets to Ag(110) is unlikely to improve the energetic stability.

Having examined the Ag[100] wires, we now examine Ag(111)[110] and Ag(001)[110] wires (figure 4) with a CSL interface. As discussed later, the Ag(111) wires are particularly stable compared to the others. The Ag(111) wires consist of close-packed atomic planes that have a CSL match with the substrate, and thus experience no visible deformation (figures 4(a)–(c)). As indicated in figure 4(a) for the Ag(111) monolayer, however, those Ag–Ag bonds

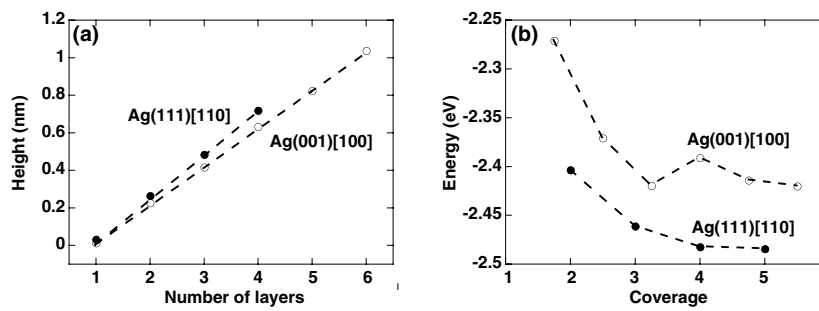


**Figure 5.** (a) Variation of height with the number of layers. Dashed lines have the slope of a bulk interplanar spacing. (b) Variation of energy  $E_a$  with thickness. (Coverage is taken as abscissa to facilitate comparison between different types of wire.)

that are in register with the Bi dimers are slightly elongated to 0.302 nm. The bonds remain elongated (0.311 and 0.310 nm) even in the base layers of the 2–4 L wire. Apart from this subtle change, the Ag(111) wires have a bulklike structure. Electronically, the Ag(111) monolayer shows the character of a metallic wire; as the band structure along the wire direction (figure 4(f)) shows, partially filled bands lie within the energy gap of the substrate.

The Ag(001)[110] 3 L wire (figure 4(d)) also has a bulklike structure. This wire has the same coverage (2.0) and the same number of atoms (eight atoms per Bi nanoline cell) on the Ag(111) facets as the Ag(111) 2 L wire; however, its base layer (0.57 nm wide) is wider than the Ag(111) base layer (0.51 nm wide), and thus does not fit so well to the underlying row of Si–Si bonds (0.24 nm wide). This wire correspondingly has a higher energy (–2.39 eV) than the Ag(111) 2 L wire (–2.46 eV).

Using the base layer of the Ag(001)[110] 3 L wire as a starting geometry, we also calculated the optimized geometry of the Ag(001)[110] monolayer shown in figure 4(e). This monolayer, not being a close-packed plane, undergoes extensive changes, becoming partly close packed. Despite this deformation, its energy (–2.32 eV) is still higher than that (–2.40 eV) of the Ag(111) monolayer.

Having examined the geometry of various wires, we now discuss the variation of height and energy  $E_a$  with thickness (figure 5). (For simplicity, figure 5 shows data only for the Ag(001)[100] and Ag(111)[110] wires.) As described above, the Ag wires have bulklike structure. The heights of the wires are thus very close to multiples of a bulk interplanar spacing, as can be seen in figure 5(a). This facilitates the identification of the orientation of a wire in experiment. As can be seen in figure 5(b), the Ag(111)[110] wires, having an excellent CSL match to the substrate, are particularly stable compared to the others. The energy  $E_a$  of the Ag(111) wire decreases asymptotically as the thickness increases, suggesting that Ag forms three-dimensional nuclei on the Bi nanoline instead of growing layer by layer. Thus, to allow the nuclei to grow along the Bi nanoline to form long wires, it is at least necessary to suppress secondary nucleation on their top facets. The energy  $E_a$  of the Ag(001) wire also decreases asymptotically as the coverage increases, except that the 3 L wire is more stable than the 4 L wire. This reversal is advantageous in growing wires with fixed height.

#### 4. Summary

The geometry and energy of the epitaxial Ag nanowires growing on the Bi nanoline have been calculated at the GGA level. The wires examined include the Ag(001)[100] and Ag(110)[100]

wires with Ag(001) facets, and the Ag(111)[110] and Ag(001)[110] wires with Ag(111) facets. We have found that the Ag wires other than Ag(001) monolayers have a bulklike structure. The calculated heights of the wires are thus very close to multiples of interplanar spacings. The calculated electronic band structure indicates that the wires are metallic or semimetallic. Among the wires examined, the Ag(111) wires with a CSL interface with the Bi nanoline are particularly stable. The energetic stability of the Ag wire generally improves as the thickness increases, indicating that Ag grows through three-dimensional nucleation on the Bi nanoline.

### Acknowledgments

The calculations were performed using the Numerical Materials Simulator at NIMS and the NEC SX-5 at Cyber Media Centre, Osaka University. HK is supported by the JSPS Research Fellowships for Young Scientists. This work is in part supported by a Grant-in-Aid from the Ministry of Education, Culture, Sports, Science and Technology.

### References

- [1] Bowler D R 2004 *J. Phys.: Condens. Matter* **16** R721
- [2] Miki K, Bowler D R, Owen J H G, Briggs G A D and Sakamoto K 1999 *Phys. Rev. B* **59** 14868
- [3] Naitoh M, Shimaya H, Nishigaki S, Oishi N and Shoji F 1997 *Surf. Sci.* **377–379** 899
- [4] Owen J H G and Miki K 2006 *Surf. Sci.* **600** 2943
- [5] Owen J H G and Miki K 2006 *Nanotechnology* **17** 430
- [6] Itoh T, Kashirajima S, Naitoh M, Nishigaki S and Shoji F 2005 *Appl. Surf. Sci.* **244** 161
- [7] Bowler B R and Owen J H G 2002 *J. Phys.: Condens. Matter* **14** 6761
- [8] Orellana W and Miwa R H 2006 *Appl. Phys. Lett.* **89** 093105
- [9] Koga H and Ohno T 2006 *Phys. Rev. B* **74** 125405
- [10] Koga H and Ohno T 2006 submitted
- [11] LeGoues F K, Liehr M, Renier M and Krakow W 1988 *Phil. Mag. B* **57** 179
- [12] Markov I V 2003 *Crystal Growth for Beginners* (Singapore: World Scientific) p 464
- [13] Stoyanov S 1986 *Surf. Sci.* **172** 198
- [14] Grabow M H and Gilmer G H 1988 *Surf. Sci.* **194** 333
- [15] Perdew J P, Burke K and Ernzerhof M 1996 *Phys. Rev. Lett.* **77** 3865
- [16] Hohenberg P and Kohn W 1964 *Phys. Rev.* **136** B864
- [17] Kohn W and Sham L J 1965 *Phys. Rev.* **140** A1133